FACTA UNIVERSITATIS
Series: **Automatic Control and Robotics** Vol. 12, N° 2, 2013, pp. 75 - 88

PLANE WAVE COUPLING TO HORIZONTAL WIRE ABOVE LOSSY SOIL
Comparison of Electromagnetic, Complex Image and Transmission Line Models

UDC (537.8+621.332.43):621.316.99

Vesna Arnautovski-Toseva, Leonid Grcev

Faculty of Electrical Engineering and Information Technologies,
Ss. Cyril and Methodius University, Skopje, Macedonia

Abstract. *The paper presents modeling of TM plane coupling to horizontal thin-wire conductor above homogeneous lossy soil. The main purpose of this work is to compare results of the current distribution obtained by using two approximate approaches based on: complex image theory and transmission line theory with respect to a rigorous electromagnetic approach. A detailed parametric analysis clearly illustrates the validity domain and possible limitations of approximate models in EMC studies.*

Key words: *plane wave coupling, electromagnetic theory, transmission line theory, complex image theory, homogeneous lossy soil*

1. INTRODUCTION

The electromagnetic field coupling to overhead wires has been analyzed in many electromagnetic compatibility (EMC) studies. Different strategies for modeling have been developed, ranging from transmission line theory to an exact approach based on electromagnetic theory [1-3]. In this paper the authors compare two approaches of modeling an electric field coupling to overhead wires. The first approach is based on transmission line (TL) theory by using three formulations for per unit length impedance based on [9, 10]: 1) Bridges's integral formulation; 2) Sunde's integral formulation; and 3) Sunde's approximate logarithmic Formulation. The complex image model is based on a complex image approximation of the Green's functions that arises in the electromagnetic model. The verification is done by comparison with the results obtained by electromagnetic (EM) model which is based on Method of Moments (MoM) solution

Received November 27, 2013
Corresponding author: Vesna Arnautovski-Toseva
Faculty of Electrical Engineering and Information Technologies, Ss. Cyril and Methodius University, Karpos II, 1000 Skopje, Macedonia
E-mail: atvesna@feit.ukim.edu.mk

of the exact Mixed Potential Integral Equation (MPIE) for the electric field. The main purpose of this work is to analyze the domain of applicability of the derived approximate models for the use in EMC studies.

2. MATHEMATICAL MODELS

2.1. Physical model

We consider *x*–directed horizontal thin-wire conductor of radius *a* and length *L* located at height *h* above lossy soil, as shown in Fig. 1. The air (medium 0) is characterized by permeability μ_0, and permittivity ε_0. The homogeneous lossy soil (medium 1) is characterized by permeability μ_0, permittivity $\varepsilon_1=\varepsilon_r\varepsilon_0$ and conductivity σ_1. The wire is illuminated by a uniform plane wave of normal incidence and $e^{j\omega t}$ time dependency with electric field vector defined by $\boldsymbol{E}^i = \hat{i}_x E_0 e^{jk_0 z}$.

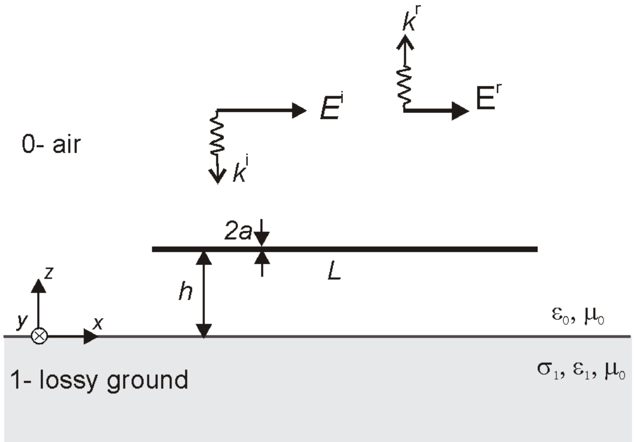

Fig. 1 Horizontal wire above lossy soil illuminated by a plane wave of normal incidence

2.2. Electromagnetic model

The electromagnetic model (EM) [4] is used as a referent model. It is based on a full-wave theory, more particularly, on the integral formulation of the electric field due to filaments of current and charge induced along the axis of the conductor, which is solved by using Galerkin formulation of method of moments with roof-top bases and test functions along overlapping wire segments of length l_n. The boundary conditions regarding the tangential component of the electric field at the wire surface are satisfied approximately in an average (weighted) way.

The current distribution is obtained by solving the following matrix equation $[I] = [Z]^{-1}[U]$, where $[Z]$ is a generalized impedance matrix, and $[U]$ is excitation matrix. Fig. 2 shows simplified approximation of the current with roof-top basis functions and the excitation matrix model $[U]$. The elements of matrix $[U]$ are determined by

$$U_n = \int_{l_n} E dl_n \; ; \quad E = E^i + E^r \, , \tag{1}$$

where E is the total electric field, sum of the incident and reflected field, tangential to the wire-conductor.

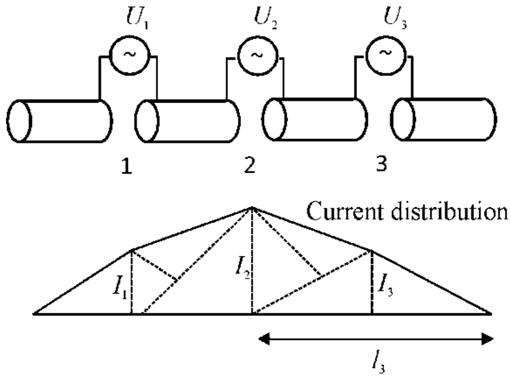

Fig. 2 Modeling of the excitation in the mathematical model

The elements of matrix [Z] are defined by

$$z_{mn} = \frac{1}{I_n} \int_{l_m} [\, j\omega \int_{l_n} G_A^{xx} I_n dl_{nx} + \frac{\partial}{\partial x} \int_{l_n} G_V q_n dl_{nx} \,] \, dl_m \, , \tag{2}$$

where G_A^{xx} is x–component of the dyadic Green's function for the magnetic vector potential, and G_V is scalar potential Green's function for the given problem [5, 6]:

$$\begin{aligned} G_A^{xx} &= \frac{\mu_0}{2} \left[G_{dir} + \frac{1}{2\pi} \int_0^\infty R_{TE} \frac{e^{-u_0(z+z')}}{u_0} J_0(\lambda\rho) \lambda d\lambda \right] \\ G_V &= \frac{1}{2\varepsilon_0} \left[G_{dir} + \frac{1}{2\pi} \int_0^\infty \frac{k_0^2 R_{TE} - u_0^2 R_{TM}}{\lambda^2} \frac{e^{-u_0(z+z')}}{u_0} J_0(\lambda\rho) \lambda d\lambda \right] \end{aligned} . \tag{3}$$

The integrals in (3) are of Sommerfeld type where $J_0(\lambda\rho)$ is zero-order Bessel function of the first kind. The solution of Sommerfeld integrals is obtained by direct numerical integration similarly to the approach in [3].

The term G_{dir} in (3) is so called direct term that represents a spherical wave radiated from horizontal electric dipole (HED) located at (0, 0, z') in unbounded free space (air) with respect to the observation point in (x, y, z), where ρ is a radial distance between the source HED and the observation point

$$G_{dir} = \frac{e^{-jk_0\sqrt{\rho^2 + |z-z'|^2}}}{2\pi\sqrt{\rho^2 + |z-z'|^2}} = \frac{e^{-jk_0 R_{dir}}}{2\pi R_{dir}} \, . \tag{4}$$

In (3) the Fresnel reflection coefficients are

$$R_{TE} = \frac{u_0 - u_1}{u_0 + u_1} \qquad R_{TM} = \frac{k_1^2 u_0 - k_0^2 u_1}{k_1^2 u_0 + k_0^2 u_1}\,, \tag{1}$$

where

$$\begin{aligned} &u_i = \sqrt{\lambda^2 - k_i^2}; \quad i = 0,1 \\ &k_0^2 = \omega^2 \mu_0 \varepsilon_0; \quad k_1^2 = \underline{\varepsilon}_r k_0^2 \quad \underline{\varepsilon}_r = \varepsilon_r - j\sigma(\omega\varepsilon_0)^{-1}. \end{aligned} \tag{2}$$

This model is assumed with at least approximations that arise due numerical calculation procedures for solving Sommerfeld integrals that arise in the rigorous formulation (3).

2.3. Complex image model

The complex image model (Cimg) is based on quasi-static approximation $u_0 \approx \lambda$ and Wait-Spies [7] and Bannister's [8], where $d = 2[\,j\omega\mu_0\,(\sigma_1 + j\omega\varepsilon_1)]^{-1/2}$ is complex depth. By this, we obtain the following approximation

$$R_{TE} \to \frac{\lambda - u_1}{\lambda + u_1} \approx -e^{-\lambda d} \approx -e^{-u_0 d}\ ; \quad R_{TM} \to K = \frac{k_1^2 - k_0^2}{k_1^2 + k_0^2}\,. \tag{3}$$

This leads to the following approximate expressions that are easily solved in a closed form

$$\begin{aligned} G_A^{xx} &= \frac{\mu_0}{2}\left[G_{dir} - \frac{1}{2\pi}\int_0^\infty \frac{e^{-u_0[(z+z')+d]}}{u_0} J_0(\lambda\rho)\lambda d\lambda\right] \\ &= \frac{\mu_0}{4\pi}\left[\frac{e^{-jk_0 R_{dir}}}{R_{dir}} - \frac{e^{-jk_0\sqrt{\rho^2+(z+z'+d)^2}}}{\sqrt{\rho^2+(z+z'+d)^2}}\right] = \frac{\mu_0}{2}\left[G_{dir} - G_{Cimg}\right] \\ G_V &= \frac{1}{4\pi\varepsilon_0}\left[\frac{e^{-jk_0 R_{dir}}}{R_{dir}} - \frac{Ke^{-jk_0\sqrt{\rho^2+(z+z')^2}}}{\sqrt{\rho^2+(z+z')^2}}\right] = \frac{1}{2\varepsilon_0}\left[G_{dir} - KG_{img}\right]. \end{aligned} \tag{4}$$

The term G_{Cimg} in G_A^{xx} corresponds to the field of the so called complex image of the HED located at complex depth (0, 0, $-(z' + d)$) [7]. In G_V the term G_{img} represents the spherical field of the image of the source HED at (0, 0, $-z'$).

2.4. Transmission line model

The transmission line (TL) equations for a horizontal thin-wire conductor above lossy soil excited by electric field plane wave of normal incidence can be derived from the Maxwell's equations and expressed in terms of voltage and current induced along the conductor [2]

$$\frac{\partial V(x)}{\partial x} + ZI(x) = E(x,h); \quad \frac{\partial I(x)}{\partial x} + YV(x) = 0\,, \tag{5}$$

where per unit length impedance Z and admittance Y are defined by:

- Bridges's integral formulation

$$Z=\frac{j\omega\mu_0}{2\pi}\left[K_0(k_0a)-K_0(k_0[2h-a])+2\int_0^{\infty}\frac{e^{-2hu_1}}{\lambda+u_1}d\lambda\right]$$
$$Y=\frac{j\omega 2\pi\varepsilon_0}{K_0(k_0a)-K_0(k_0[2h-a])+2\int_0^{\infty}\frac{e^{-2hu_1}}{\frac{k_1^2}{k_0^2}\lambda+u_1}d\lambda} \tag{6}$$

- Sunde's integral formulation

$$Z=\frac{j\omega\mu_0}{2\pi}\left[\ln\frac{2h}{a}+2\int_0^{+\infty}\frac{e^{-2\lambda h}}{\lambda+u_1}d\lambda\right]$$
$$Y=\frac{j\omega 2\pi\varepsilon_0}{\ln\frac{2h}{a}+2\int_0^{+\infty}\frac{e^{-2\lambda h}}{\frac{k_1^2}{k_0^2}\lambda+u_1}d\lambda} \tag{7}$$

- Sunde's integral formulation

$$Z=\frac{j\omega\mu_0}{2\pi}\left[\ln\frac{2h}{a}+\ln\frac{1+\gamma_1 h}{\gamma_1 h}\right]$$
$$Y=\frac{j\omega 2\pi\varepsilon_0}{\ln\frac{2H}{a}}\,\|\,Y_g;\qquad Y_g=\frac{\gamma_1^2}{Z_g} \tag{8}$$

The solution for the current distribution is obtained by

$$I(x)=\frac{E}{Z_0}\frac{(1-e^{\gamma_1 L})e^{-\gamma_1 x}}{(e^{\gamma_1 L}-e^{-\gamma_1 L})}+\frac{-E}{Z_0}\frac{(1-e^{-\gamma_1 L})e^{\gamma_1 x}}{(e^{\gamma_1 L}-e^{-\gamma_1 L})}+\frac{E}{Z_0}, \tag{9}$$

where $Z_0=\left[ZY^{-1}\right]^{\frac{1}{2}}$ is the characteristic impedance, and $\gamma_1=\left[ZY\right]^{\frac{1}{2}}=jk_1$.

3. Numerical Results

To examine the domain of applicability of the presented approximate models we have compared the current induced along a horizontal conductor above lossy soil excited by a plane wave of normal incidence. The results obtained by using the EM model are used as reference.

The studied cases are: L = 20-m and L = 200-m horizontal conductors located at height h: 0.1 m; 0.5 m, 1 m, and 3 m above homogeneous lossy soil with ε_r = 10. The soil conductivity σ_1 is: (low) 0.001 S/m; (medium) □0.01 S/m; and (high) 0.1 S/m. The excitation is TM plane wave of normal incidence E^i = 1 V/m in frequency range from 0.01 to 10 MHz.

The accuracy of the approximate models with respect to EM model is measured by the rms current distribution error [11]

$$\varepsilon_{rms} = \left[\frac{\sum_{i=1}^{N} \left| \underline{I}_{EMi} - \underline{I}_{approxi} \right|^2}{\sum_{i=1}^{N} \left| \underline{I}_{EMi} \right|^2} \right]^{1/2} \cdot 100\,(\%)\,, \tag{10}$$

where $\underline{I}_{EMi}$ and $\underline{I}_{approxi}$ are phasors of the current samples along the conductor computed by EM model and by using both TL and the Cimg approximate models. N is number of samples (basis functions).

3.1. 20-m horizontal conductor

Fig. 3 shows variations of the current magnitude at the centre of a 20-m wire- conductor at heights h: 0.1 m, 0.5 m, 1 m and 3 m above homogeneous soil (σ_1 = 0.01S/m) calculated by EM model. As may be observed, the maximum of the current magnitude at the resonant frequency increases when the wire height h decreases.

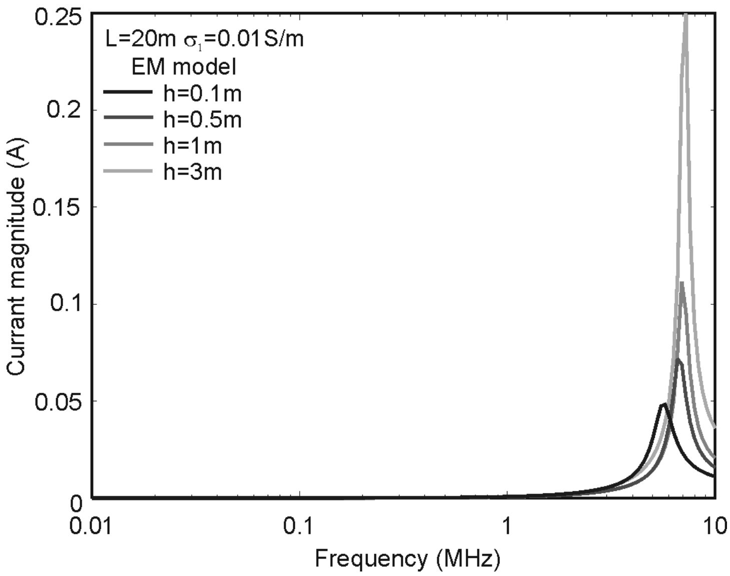

Fig. 3 Magnitude of the current in the centre of a 20-m wire at various height h above lossy soil (σ_1=0.01S/m)

In Fig-s. 4, 5, 6 and 7 the corresponding ε_{rms} error (10) may be observed. The results clearly show that the applicability of the approximate models (TL and Cimg) is very sensitive for frequencies around the resonant when maximal ε_{rms} errors are obtained.

As may be observed, all TL models introduce ε_{rms} error that varies from 20% to >100% at the resonant frequency. At low frequencies ε_{rms} error varies from 2% (when h = 0.1 m) to 10% (when h = 3 m).

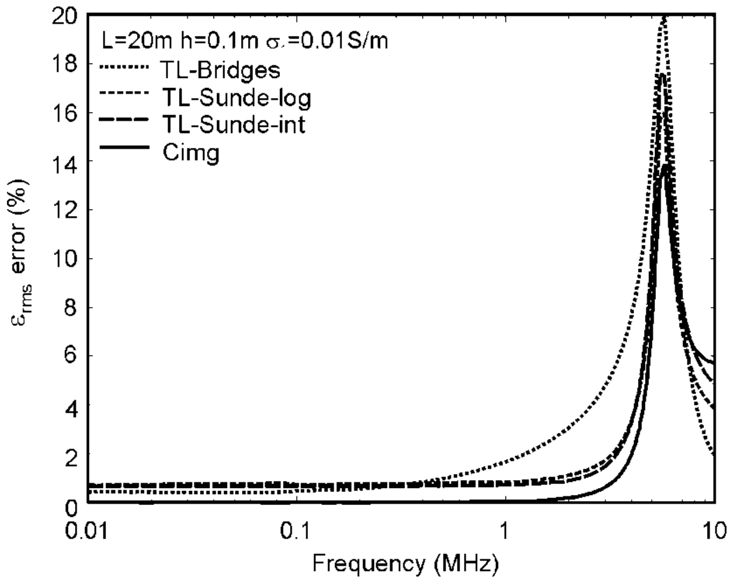

Fig. 4 ε_{rms} error of the current along a 20-m wire at 0.1 m above lossy soil (σ_1=0.01S/m)

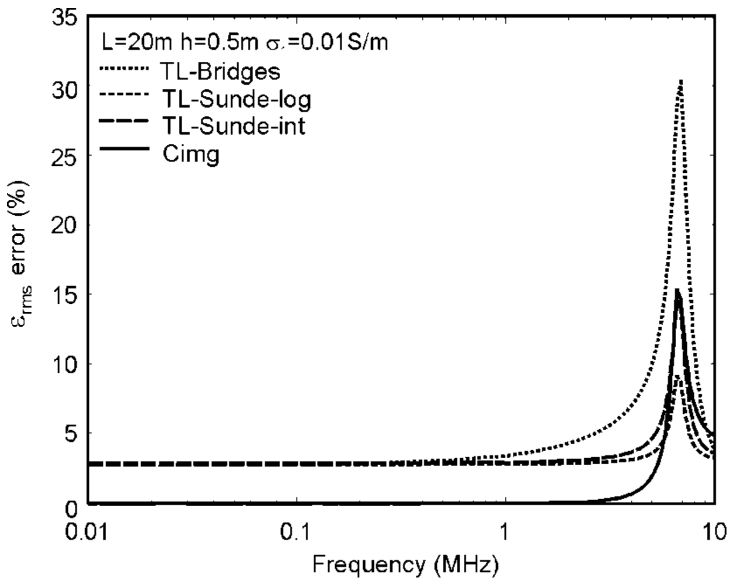

Fig. 5 ε_{rms} error of the current along a 20-m wire at 0.5 m above lossy soil (σ_1=0.01S/m)

The Cimg model introduces ε_{rms} error which is in range (10 - 15)% at the resonant frequency. For other frequencies the ε_{rms} error is less than 2%. It may be observed that the height *h* has no significant influence on the accuracy of the Cimg model.

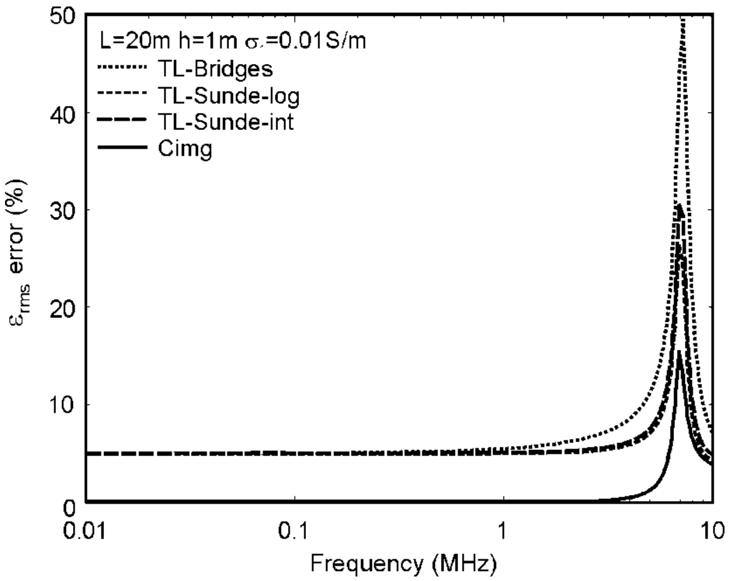

Fig. 6 ε_{rms} error of the current along a 20-m wire at 1 m above lossy soil (σ_1=0.01S/m)

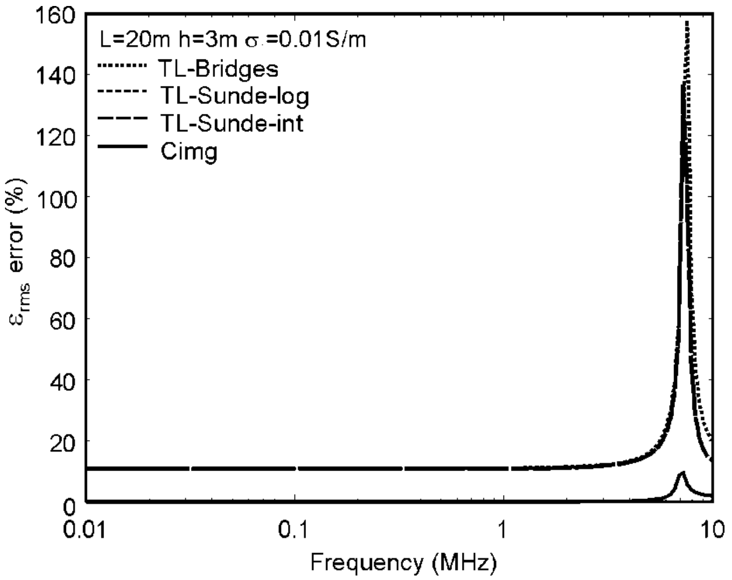

Fig. 7 ε_{rms} error of the current along a 20-m wire at 3 m above lossy soil (σ_1=0.01S/m)

Next, in Fig-s. 8 and 9 it is shown that the ε_{rms} error calculated in the case when the 20-m conductor is at height h = 3 m above low conductive soil (σ_1 = 0.001S/m) and high conductive soil (σ_1 = 0.1S/m).

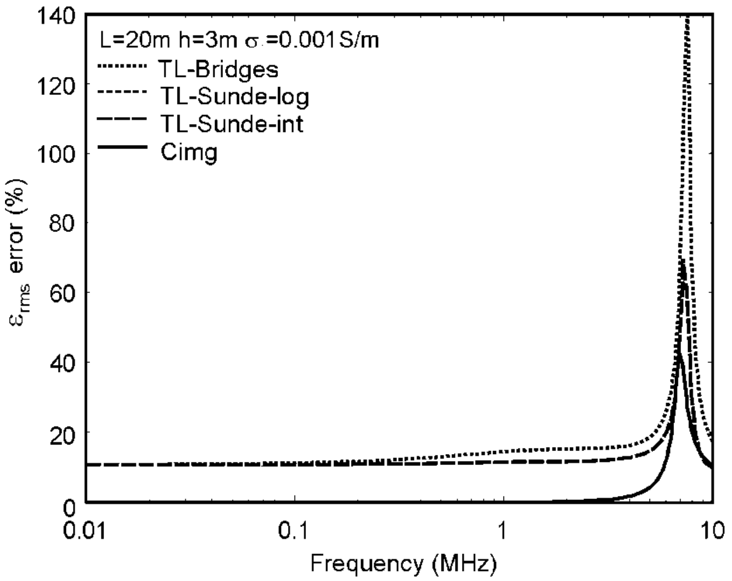

Fig. 8 ε_{rms} error of the current along a 20-m wire at height 3 m above soil (σ_1=0.001S/m)

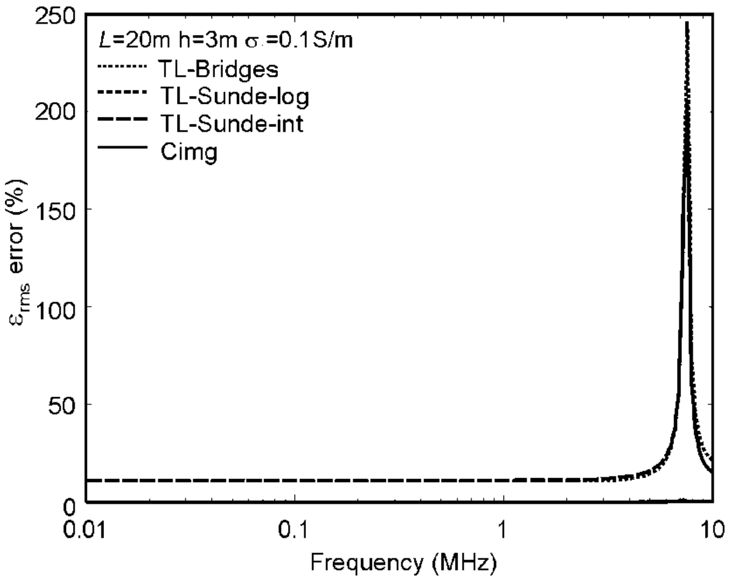

Fig. 9 ε_{rms} error of the current along a 20-m wire at height 3 m above soil (σ_1=0.1S/m)

As may be observed, the accuracy of all models is dependent on the soil conductivity. The ε_{rms} error due to Cimg model is practically below 1% in all frequency ranges when the soil is highly conductive. However, when the soil is low conductive, the ε_{rms} error increases (around 40%). TL models also show better accuracy when the conductivity is high for frequencies out of resonances. Again, for the resonant frequency the peak of the ε_{rms} error increases (200% when σ_1 = 0.1S/m)

3.2. 200-m horizontal conductor

Similarly as previous, Fig. 10 shows the changes of the current magnitude at the centre of a 200-m wire at heights *h* from 0.1 m to 3 m above lossy soil (σ_1=0.01S/m) with respect to frequency.

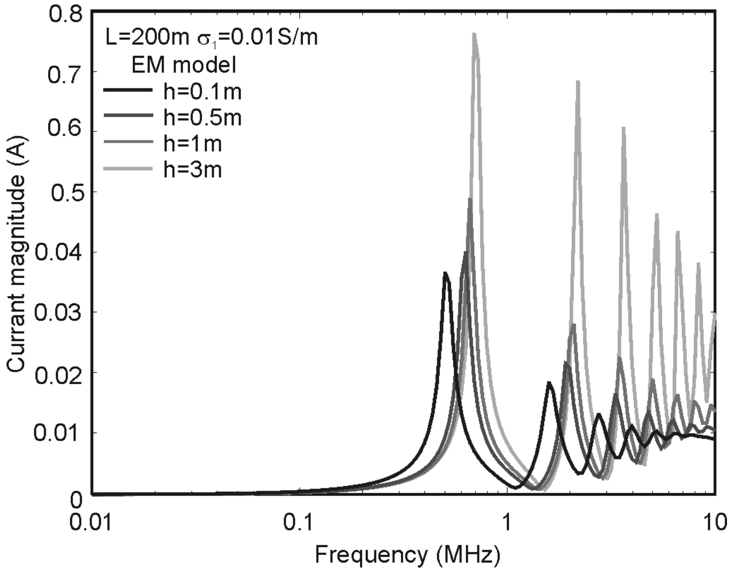

Fig. 10 Magnitude of the current in the centre of a 200-m wire at various height *h* above lossy soil (σ_1=0.01S/m)

The corresponding ε_{rms} error is shown in Fig-s. 11, 12, 13 and 14. The results confirm the previous conclusions that the accuracy of approximate models is strongly dependent on resonant frequencies when maximal ε_{rms} error occurs. All TL models show much better accuracy when the conductor is close to the soil surface, whereas Cimg models show almost no dependence with respect to the wire height *h*. When the wire is long, the peaks of the ε_{rms} error are within 15%.

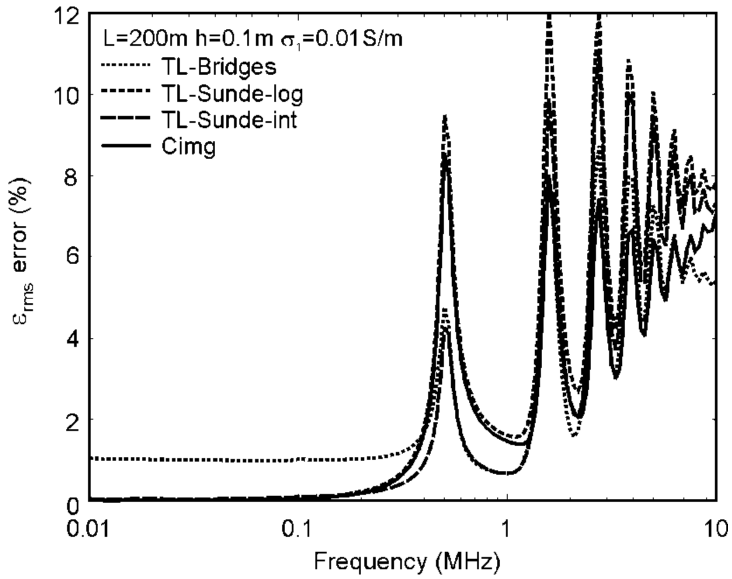

Fig. 11 ε_{rms} error of the current along a 200-m wire at 0.1 m above lossy soil (σ_1=0.01S/m)

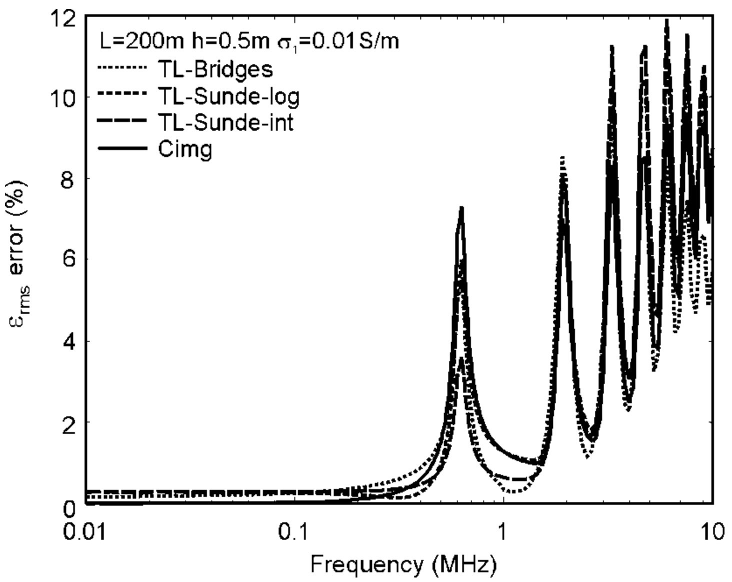

Fig. 12 ε_{rms} error of the current along a 200-m wire at 0.5 m above lossy soil (σ_1=0.01S/m)

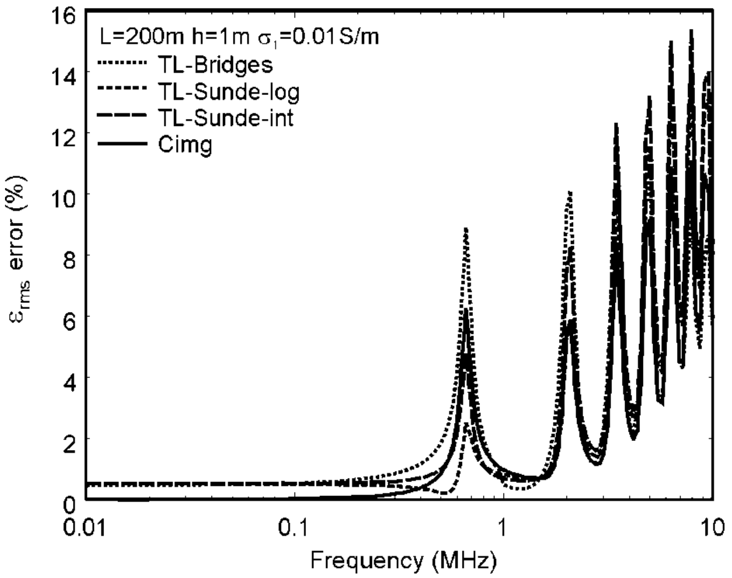

Fig. 13 ε_{rms} error of the current along a 200-m wire at 1 m above lossy soil (σ_1=0.01S/m)

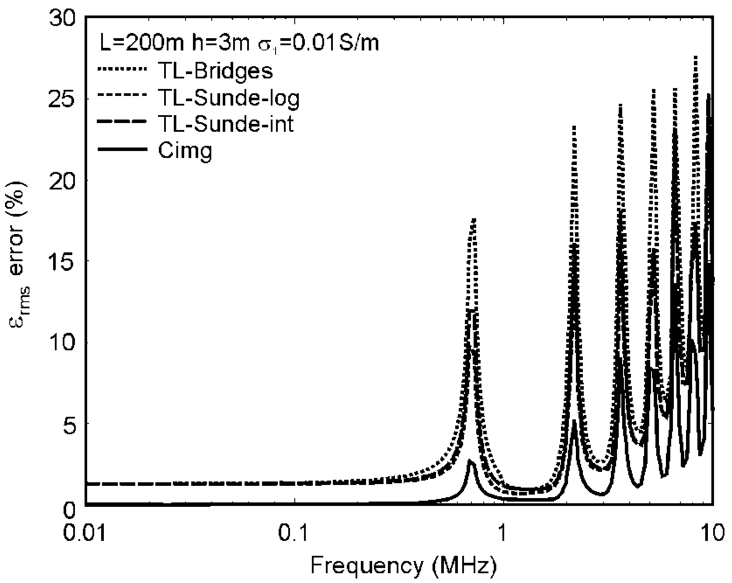

Fig. 14 ε_{rms} error of the current along a 200-m wire at 3 m above lossy soil (σ_1=0.01S/m)

The influence of the soil conductivity on the accuracy of TL and Cimg models in case of a long wire is shown in Fig-s. 15 and 16. As may be observed in case of high conductive soil (Fig. 16) the calculation error of Cimg model is within 2% for all studied frequencies. The peaks of ε_{rms} error due to Cimg model decrease when increasing the soil conductivity. Contrary, the peaks of ε_{rms} error due to TL models increase when decreasing the soil conductivity.

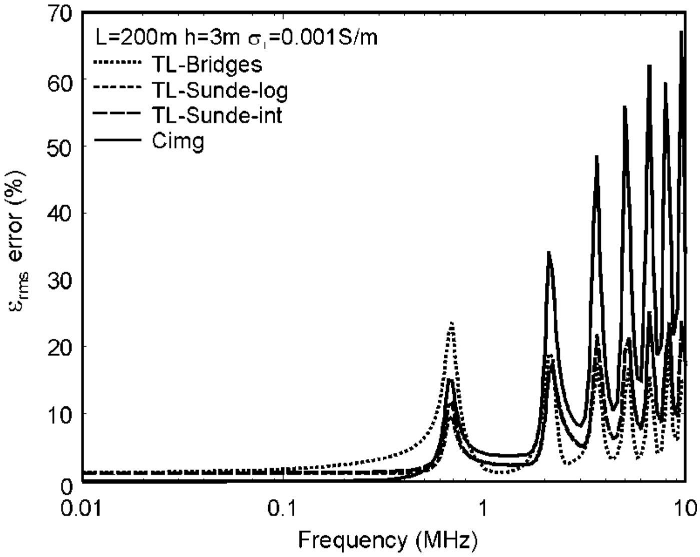

Fig. 15 ε_{rms} error of the current along a 200-m wire at height 3 m above soil (σ_1=0.001S/m)

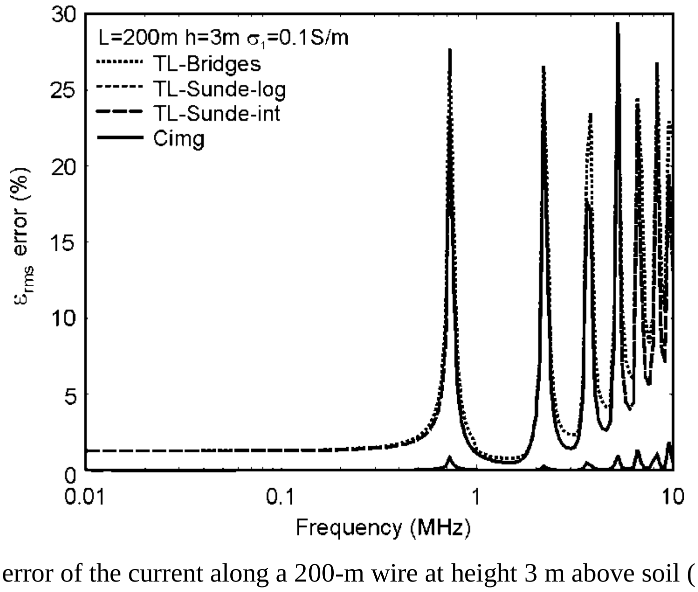

Fig. 16 ε_{rms} error of the current along a 200-m wire at height 3 m above soil (σ_1=0.1S/m)

4. Conclusion

The EM modeling of high frequency behavior of wire conductors in the presence of lossy soil is considered as numerically most precise. However, in the EMC studies in practice, often most simplified models are needed. In this paper the authors analyze the accuracy of two approximate approaches: Cimg (complex image) model and three variations of TL (transmission line) model. The results of the rms current distribution error may be summarized in:

- The accuracy of Cimg and TL models show strong dependence on the resonant frequencies.
- The Cimg model shows very good agreement with the reference EM model ε_{rms} error < 10-15% at resonant frequencies), except when the soil is low conductive (σ_1=0.001S/m). The peaks of the ε_{rms} error decreases when increasing the soil conductivity.

The TL models show good agreement for medium to highly conductive soil, and when the conductor is close to the soil surface. Otherwise, the ε_{rms} error at resonant frequencies might be very high. The peaks of the ε_{rms} error increase when increasing the soil conductivity.

References

[1] F. Rachidi, S. Tkachenko, *Electromagnetic Field Interaction with Transmission Lines*, WIT Press, 2008.

[2] F. M. Tesche, M. Ianosz, T. Karlsson, *EMC Analysis Methods and Computational Models*, John Wiley and Sons, 1997.

[3] G.J. Burke, E.K.Miller, "Modeling antennas near to and penetrating a lossy interface," IEEE Trans. Antennas Propagation, vol. AP-32, no. 10, pp. 1040–1049, 1984. [Online]. Available: http://dx.doi.org/10.1109/TAP.1984.1143220

[4] V. Arnautovski-Toseva, K. El Khamlichi Drissi, K. Kerroum, "Comparison of approximate models of horizontal wire conductor above homogeneous ground," in *Proceedings of 6th European Conference on Antennas and Propagation, EUCAP 2012*, Prague, pp. 1–5, 2012. [Online]. Available: http://dx.doi.org/10.1109/EuCAP.2012.6205956

[5] J. R. Mosig, "Integral equation technique" in *Numerical Techniques for Microwave and Milimeter-Wave Passive Structures*, New York: Wiley, 1989, pp. 133–213.

[6] K. A. Michalski, "The mixed-potential electric field integral equation for objects in layered media," Archiv Elektronik und Uebertragungstechnik, vol. 39, no. 5, pp. 317–322, 1985.

[7] J. R. Wait, K. P. Spies, "On the image representation of the quasi-static fields of a line current source above the ground," Canadian Journal of Physics, vol. 47, no. 23, pp. 2731–2733, 1969. [Online]. Available: http://dx.doi.org/10.1139/p69-334

[8] P. Bannister, "Applications of complex image theory," Radio Science, vol. 21, no. 4, pp.605–616, 1986.

[9] E. D. Sunde, *Earth Conduction Effects in Transmission Systems*, Dover publication, New York, 1968.

[10] N. Theethayi, R. Thottappillil, "Surge propagation and crosstalk in multiconductor transmission lines above ground," in *Electromagnetic Field Interaction with Transmission Lines*, WIT Press, 2008.

[11] Poggio, R. Bevensee, E.K. Miller, "Evaluation of some thin wire computer programs," in *Proceedings of IEEE Antennas and Propagation Symposium*, vol. 12, pp. 181–184, 1974. [Online]. Available: http://dx.doi.org/10.1109/APS.1974.1147236